A Quantitative Description of the Effect of Process Conditions on the Physical Structure of Poly(ethylene Terephthalate) Yarns with an Application to Dyeing Behavior

R. HUISMAN and H. M. HEUVEL, *Fiber Research Department, Akzo Research Laboratories Arnhem, The Netherlands*

Synopsis

The intrinsic properties of a yarn are brought about by its physical structure. This structure in its turn is controlled by the process conditions applied. A quantitative description is given of the effect of temperature, time, and tension during annealing on the structure of poly(ethylene terephthalate) yarns. Annealing of a yarn at elevated temperature leads to improvement of packing of the molecules within the crystals. Consequently, the crystalline density is not a constant but is largely dependent on the conditions under which crystallization has taken place. The growth of the PET crystals is not an isotropic process; the strongest growth is observed in the direction of the dipole interactions. The effects of tension and annealing time are also discussed. A prolonged annealing time causes an increase in crystallinity, while time and tension influence the growth of the crystals to some extent. However, for the experimental conditions used in this investigation, temperature is by far the most important factor. Generally speaking, PET fibers annealed at low temperature show low crystallinity built up of many small crystals. Yarn annealed at a high temperature, on the other hand, is composed of fewer big crystals together with large adjacent amorphous regions and relatively high overall crystallinity. Finally, the effect of this observed structural morphology on the dyeing behavior of PET yarns is discussed in a qualitative way. Two main effects controlling the dye uptake of PET yarn are proposed, viz., the total amount of amorphous regions and the accessibility of these regions.

INTRODUCTION

A synthetic yarn process is essentially a succession of heat treatments at a certain tension and during a defined residence time. Almost all process conditions can be reduced to these three essential factors. During the development of a process or in a later stage for process control, knowledge about the relation between the yarn properties obtained and the applied process conditions is highly desirable. However, these relations may be confused due to the complexity of the process involved. Therefore, a purely statistical approach has the permanent danger of spurious correlations.

A more reliable way, in our opinion, is to split up the mentioned relations. The applied process conditions result in a certain physical yarn structure. This structure, in its turn, is responsible for the intrinsic textile properties of the yarn. In this way, the relations observed can be supported by physical interpretation. In this physical approach, the occurrence of spurious correlations is avoided. Furthermore, process extrapolations can be made in a much more reliable way.

For the description and control of the process, quantitative information about the structural response of a yarn during the various process steps is required.

Journal of Applied Polymer Science, Vol. 22, 943–965 (1978)

0021-8995/78/0022-0943$01.00

These quantitative data can be used for comparison of yarns produced during the development of a process. They can also be used for establishing a possible correlation between different types of parameters, e.g., structural and textile parameters. For a rapid feedback in process development, at least 10 to 20 yarn samples a day should be characterized, which calls for a measurement time of less than one hour.

This paper describes an investigation into the effects of temperature, tension, and duration of heat treatment on the physical structure of PET yarns. Use is made of x-ray diffraction, density measurements, and pulse propagation to study the crystalline morphology and the orientation of the amorphous and crystalline components. The results are given in terms of an x-ray quantification model published earlier.[1] Finally, the structural picture obtained will be used for the interpretation of important differences in the dyeing behavior of PET yarns.

EXPERIMENTAL

The heat treatment used to prepare the yarns for this investigation was carried out at temperatures, tensions, and residence times similar to those encountered in practical technology. The feed yarn was spun and drawn in a conventional way. The ultimate yarns were obtained after a heat treatment of 30 and 70 msec, with the hot-plate temperature adjusted at 100°, 150°, 200°, and 250°C, respectively. During the heat treatment, two different tensions were applied, viz., 10 and 70 cN; at a yarn count of 76 dtex (24 filaments), this resulted in loads of about 1.3 and 9.2 cN/tex.

Subsequently, the structural morphology and crystalline orientation of the yarn thus produced were studied by means of wide-angle x-ray diffraction. To this end, the yarns were wound very accurately on thin sample holders and placed in a Philips diffractometer equipped with a quartz monochromomator, Soller slits, a divergence slit (1°), a scatter slit (0.2 mm), and a receiving slit (1°). To get symmetric diffraction profiles the transmission technique was used.[2] The recorded diffraction intensities were punched on paper tape for further quantitative elaboration. The calculations were performed on a CDC 6600 computer.

Densities of the yarns were determined at 23°C in a density gradient column filled with a mixture of *n*-heptane and tetrachloromethane. For the determination of the overall degree of orientation, use was made of a pulse propagation method, the propagation velocity in the yarns being measured with a dynamic modulus tester PPM-5 of H. Morgan Co. (Cambridge, Mass.).

In the dyeing experiments, equal amounts of yarn were dyed together at 125°C in one bath with a high- and a low-energy dye (i.e., a dyestuff with a large and a smaller molecule). Dyeing was carried out with 2% dyestuff calculated on weight of fiber, using 1 g/l. Setamol WS as a dispersing agent at pH 5.5. Dyeing was started at 60°C, the temperature being raised in 45 min to 125°C. At this temperature, the dyeing process was continued for 1 hr. The dyed samples were then reduction cleared at 70°C for 30 min with 1 g/l. soda ash and 2 g/l. hydrosulfite. From each yarn, the dyestuff was extracted and determined spectrophotometrically.

Use was made of Palanilbrilliantred BEL, C.J. Disperse Red 92, as a high-energy dye, and Foronblue E-BL, C.J. Disperse Blue 56, as a low-energy dye.

Quantification of X-Ray Results

In order to obtain quantitative information from the experimental diffraction patterns, the resulting profiles were simulated by symmetric bell-shaped curves. For this purpose, so-called Pearson VII lines were applied. In this approach, a single diffraction peak can be described by

$$f(x) = \frac{I_0}{[1 + 4z^2(2^{1/m} - 1)^m]}$$

where $z = (x - x_0)/H$; $f(x)$ = recorded intensity; I_0 = intensity in the center of the peak; x_0 = position of the center of the peak; H = half-width of the peak, i.e., the width at $I_0/2$; and m = shape parameter.

For $m = 1$, the well-known Lorentz (Cauchy) function is obtained; it can be proved that the Pearson VII function converts into a Gaussian one at infinite value of the shape parameter m. In general, the intensity of a composition of n (possibly overlapping) reflections together with a linear baseline (reasonable for not a too wide range of diffraction angles) can be written as

$$I = p + qx + \sum_{i=1}^{n} f_i(x)$$

From the fitted position parameters x_{0i}, information can be obtained about the packing of the molecule segments in the crystalline regions.

The half-width parameter H_i can be used in Scherrer's formula to calculate the apparent crystal size in a direction perpendicular to the crystal plane i. The expression for this apparent crystal size perpendicular to the plane i is

$$\Lambda_i^* = \lambda \frac{180}{\pi} \frac{1}{\sqrt{H_i^2 - 0.01} \cos(x_{0i}/2)}$$

where λ is the wavelength of the applied x-rays and i stands for a given set of Miller indices (hkl); the other parameters are defined as given before.

The number 0.01 used in the formula is the experimentally determined correction for the instrumental line broadening of the diffractometer.[3] In the calculation of the crystal size, no correction for lattice distortion is applied by lack of well-detectable higher-order reflections necessary for this correction.

With the help of the above-mentioned method of curve resolution, it is possible to obtain quantitative information even from overlapping reflections, together with an estimate of the standard deviation of the parameters obtained. (Those who are interested in the computer program are invited to write to the authors.) Further details of this method are published elsewhere.[1]

Method of Elaboration of the Wide-Angle X-Ray Results of PET Yarns

In order to determine the three repeat distances (axes) and the three angles of the triclinic unit cell of poly(ethylene terephthalate), the peak positions of at least six reflections should be established. A separate series of yarns was made especially for this purpose, using a heat treatment at temperatures varying from 140° to 240°C, with tensions ranging from 0.01 to 10.0 cN/tex. By means of a curve-fitting computer procedure, accurate peak positions could be determined for the reflections 010, $\bar{1}10$, 100, $0\bar{1}1$, $\bar{1}12$, $\bar{1}03$, and $\bar{1}05$. Calculation of the unit-cell dimensions with the aid of a least-squares computer procedure showed sig-

nificant variation of the length of the axes a, b, and c, whereas the angles α, β, and γ turned out to be independent of the various widely differing conditions mentioned before. The average values for the angles were found to be $\alpha = 100.1°$, $\beta = 117.9°$, and $\gamma = 110.7°$, with a standard deviation of about 0.1°. (Nomenclature according to Daubeny et al.[4])

These values are not in agreement with those formerly published by de Daubeny, Bunn, and Brown,[4] but they do agree fairly well with the results of Fakirov, Fischer, and Schmidt.[5] Also the results obtained in our company by Shuck,[6] who found $\alpha = 100.1°$, $\beta = 118.1°$, and $\gamma = 111.2°$ after refinement of 10 reflections, are in reasonable agreement with our data.

For a rapid characterization method of a yarn during the development of an industrial process, measurement of so many reflections takes too much time. Therefore, on the basis of the experience mentioned above, it was decided that the unit-cell angles would be fixed at the above values from our study. The characterization of the remaining unit-cell dimensions only requires accurate determination of the position of at least three reflections. To this end, two separate scans were performed, viz., an equatorial and a (nearly) meridional scan. The equatorial scan, ranging from 7° to 40° (2θ) contains the profiles of the reflections 010, $\bar{1}10$, and 100, together with a contribution of the amorphous regions. As the profile brought about by the amorphous phase nearly coincides with the $\bar{1}10$ reflection, only information from the two outer reflections is considered to be reliable. The meridional scan, ranging from 33° to 53° (2θ), yields the parameters of the $\bar{1}05$ reflection. At a scanning rate of 1°/min, the complete analysis of one yarn takes about 1 hr. The results of these measurements will be discussed in the continuation of this paper.

RESULTS AND DESCRIPTION OF THE CRYSTALLINE MORPHOLOGY

Unit-Cell Dimensions

For all the different settings of residence time, tension, and hot-plate temperature, the crystal structure of the yarns was characterized and unit-cell dimensions were calculated. A careful inspection of these data showed the lengths of the axes of the unit cell to be nearly independent of the duration of the heat treatment, within the range of the annealing time applied. Evidently, the growth of a PET crystal is caused by the alignment of individual molecular segments at distances which, at first approximation, only depend on the temperature and not on the size of the crystal already present.

The lengths of the cell axes a, b, and c, averaged over the two annealing times, as a function of the hot-plate temperature for the two tensions applied are given in Figures 1–3. From Figures 1 and 2, it can be seen that the lengths of the a- and b-axes decrease with increasing hot-plate temperature. This effect should be ascribed to the intrinsic behavior of the polymer molecule; due to its considerable length, the mobility of the molecular segments to be aligned to the crystal is limited. The consequence, then, is that a higher temperature, i.e., increased molecular mobility, results in a better approximation of the equilibrium distance between the molecules.

A comparison of Figures 1 and 2 shows a much stronger temperature variation

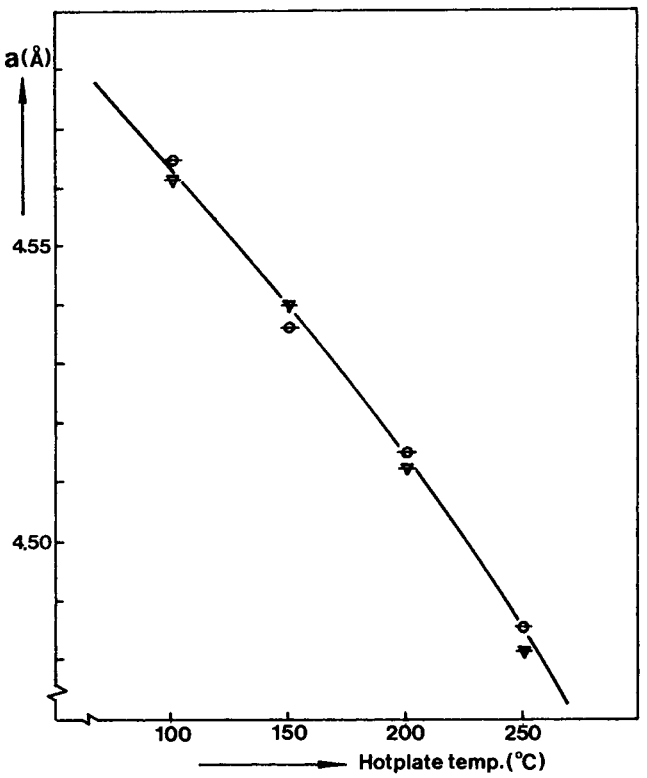

Fig. 1. a-Axis, averaged over two annealing times, as a function of hot-plate temperature at different tensions: (⊖) 1.3 cN/tex averaged over the annealing times; (▽) 9.2 cN/tex averaged over the annealing times.

of the a-axis than the b-axis. An explanation of this effect may be the strong exchange between the ester dipoles working in the b-direction, compared with the exchange between the aromatic π-electrons in the a-direction. A schematic representation of these exchange interactions, which is mentioned by several authors,[4,7,8] is given in Figure 4. Supposing that the exchange energy between neighboring molecules favors a better approach of their equilibrium distance, we may expect that a higher level of this interaction energy causes a diminished temperature dependence of the intermolecular distance.

A similar behavior is found for nylon 6, where hardly any temperature dependence of the intermolecular distance is observed in the direction of the hydrogen bonds, whereas in the other direction a very pronounced decrease of the distance is found when high temperatures are used.[9] Finally, it can be concluded from Figures 1 and 2 that the applied tension, within the range investigated, has no effect on this size of the lateral unit-cell dimensions. A substantially different behavior is found in the longitudinal direction of the unit cell. Figure 3 shows an increasing c-axis with increasing temperature for high tensions and a maximum in the curve for the lower loads.

Statton, Koenig, and Hannon[10] studied fiber structures, especially with respect to chain folding after annealing, at different levels of tension. After annealing in a relaxed state, a strong increase in chain folding was reported, whereas annealing under tension (constant length or stretching) had less or no effect.

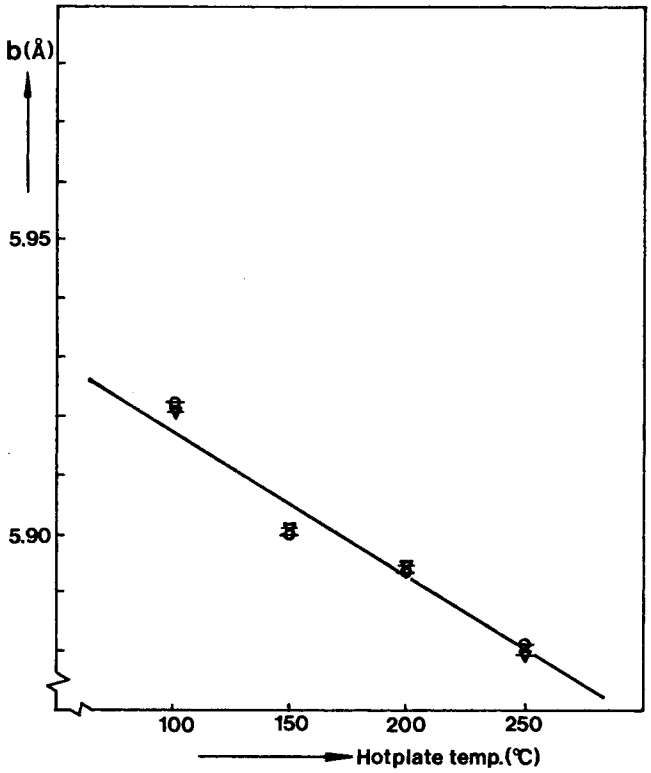

Fig. 2. *b*-Axis, averaged over two annealing times, as a function of hot-plate temperature at different tensions: (⊖) 1.3 cN/tex averaged over the annealing times; (⊽) 9.2 cN/tex averaged over the annealing times.

Combination of their experience with the observed behavior of the *c*-axis suggests that the decrease in length of the *c*-axis at high temperatures and low tension is brought about by the occurrence of chain folding, which is, of course, most effective at high temperatures. At high tensions, the applied stress is not released by chain folding, resulting in a larger *c*-axis at higher temperatures.

Crystallinity

Once the unit-cell dimensions have been determined, the crystalline density can be calculated. The crystalline density as a function of the hot-plate temperature is plotted for the two loads in Figure 5. The relatively large increase at 250°C and low tension is brought about by the mentioned contraction of the *c*-axis under these conditions. Instead of having a constant value, which according to Daubeny et al.[4] is generally assumed to be 1455 kg/m^3, the crystalline density may vary by some percentage, depending on the process conditions applied.

Such effects can only be demonstrated if a high degree of accuracy is reached in the measurements. In our opinion, digitizing of the diffractometer output followed by curve resolution offers such an opportunity. Similar effects have been observed by Hinrichsen,[11] who found a variable crystalline density for nylon 66 after a profile analysis of the equatorial reflections 100 and 010.

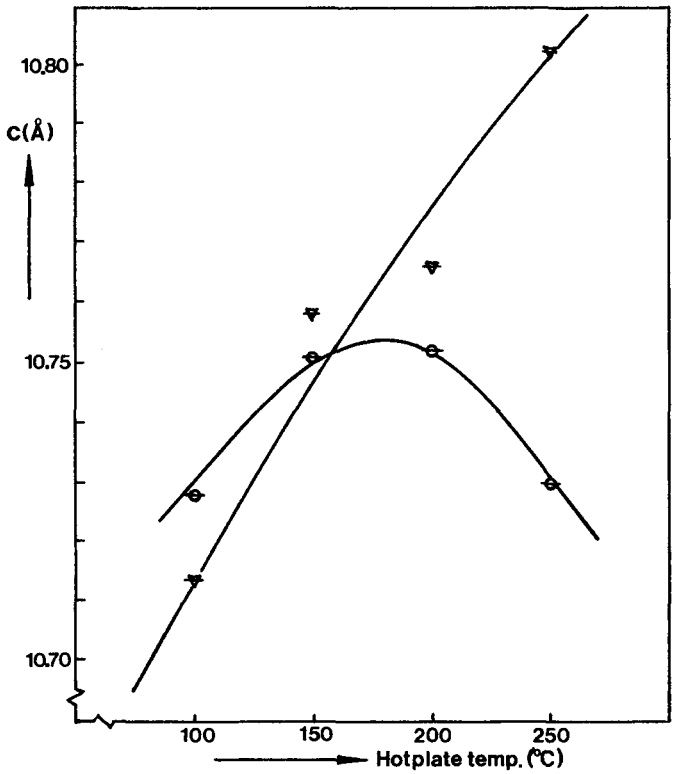

Fig. 3. c-Axis, averaged over two annealing times, as a function of hot-plate temperature at different tensions: (⊖) 1.3 cN/tex averaged over the annealing times; (▽) 9.2 cN/tex averaged over the annealing times.

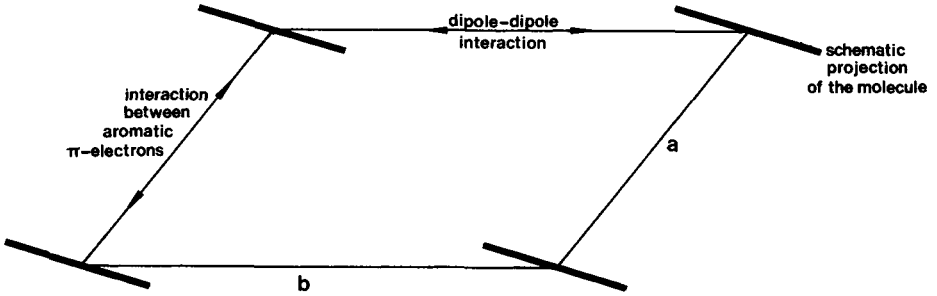

Fig. 4. Schematic cross section of the unit cell of poly(ethylene terephthalate) and representation of intermolecular interactions.

The crystalline density can be combined with the overall density determined in a gradient column and with the amorphous density in order to calculate the volume fraction of crystalline material. The amorphous density of PET is reported[4,12] to be close to 1335 kg/m^3. Also this value will not be a constant but is supposed to vary with the degree of orientation to the effect that a higher orientation results in a higher density.[12]

Therefore, a series of amorphous yarns spun at different velocities was made to obtain information about the dependence of the density on the orientation of the molecules. By means of pulse propagation, the sonic modulus was determined. According to a method to be described later under Orientation, the

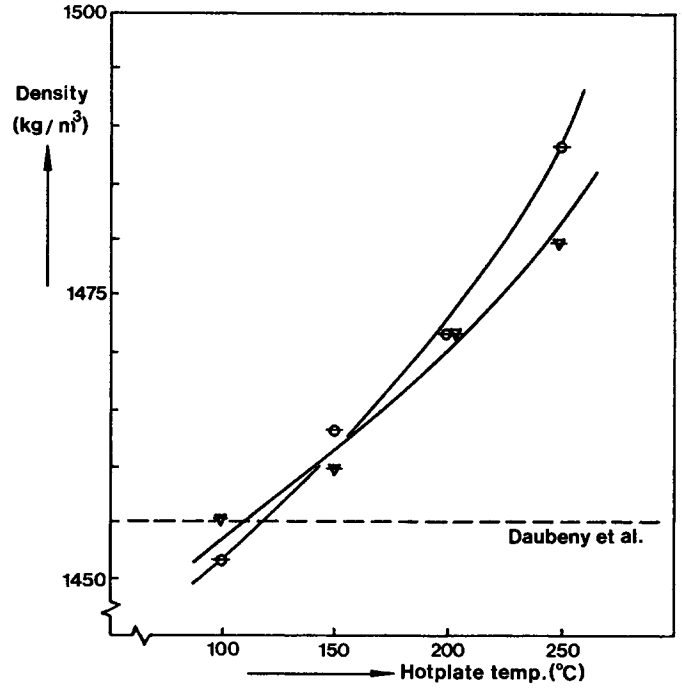

Fig. 5. Crystalline density vs. hot-plate temperature at two different loads: (⊖) 1.3 cN/tex averaged over the annealing times; (▽) 9.2 cN/tex averaged over the annealing times.

orientation factor could be determined. Figure 6 gives the relation between density and orientation designated by the orientation factor for these undrawn amorphous yarns studied. The observed variation is much smaller than the one

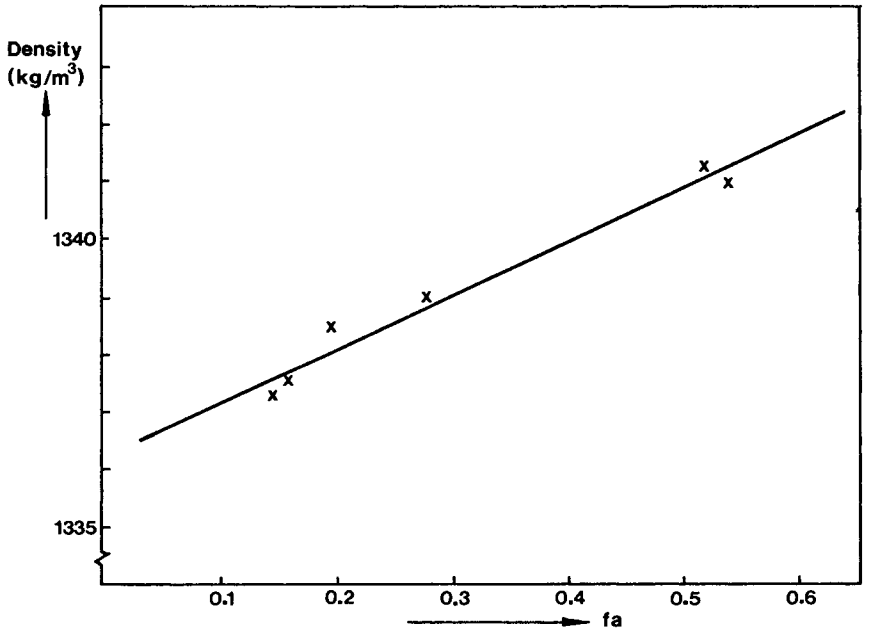

Fig. 6. Amorphous density vs orientation factor.

reported by Nobbs, Bower, and Ward.[12] The reason for this discrepancy is not clear; however, their assumption of the constant crystalline density, which they fixed at the low value of 1445 kg/m^3, is certainly not justified by our investigation.

Once the degree of orientation of the molecules in the amorphous regions has been established, the relation sketched in Figure 6 can be used to estimate the amorphous density. This procedure was applied to the series of yarns heat treated at the different temperatures (for the determination of the orientation, see "Orientation"). It was found that the variation in amorphous density over the temperature range applied is much smaller than the corresponding variation in crystalline density. This is illustrated in Figure 7, where the behavior of both crystalline and amorphous density is given for the case of heat treatment at low tension. Because of the very small variation of the amorphous density with respect to the crystalline density, it was decided that the former density be fixed at its mean value, averaged over the temperature range. So, for the calculation of the crystallinity, an amorphous density of 1342.8 kg/m^3 is used.

In Figures 8 and 9, the calculated volume fractions of crystalline material are plotted for the different settings of the variables. The crystallinity increases with increasing temperature and annealing time. Also the effect of tension is shown in the two figures. In Figure 10, the above-mentioned effect of variable crystalline density on the calculated crystallinity is demonstrated. Especially at the higher temperatures, a large discrepancy is found, leading to a lower value of the crystallinity, because the value of the actual crystalline density is much higher than 1455 kg/m^3 commonly used in the literature.[4]

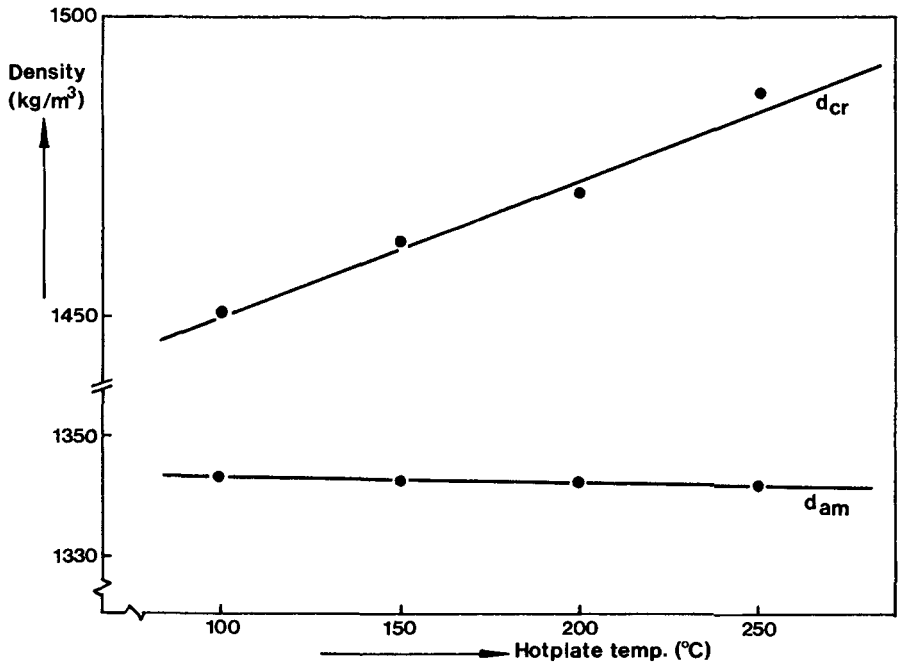

Fig. 7. Variation of crystalline and amorphous density over the applied temperature range: (●) 1.3 cN/tex, 70 msec.

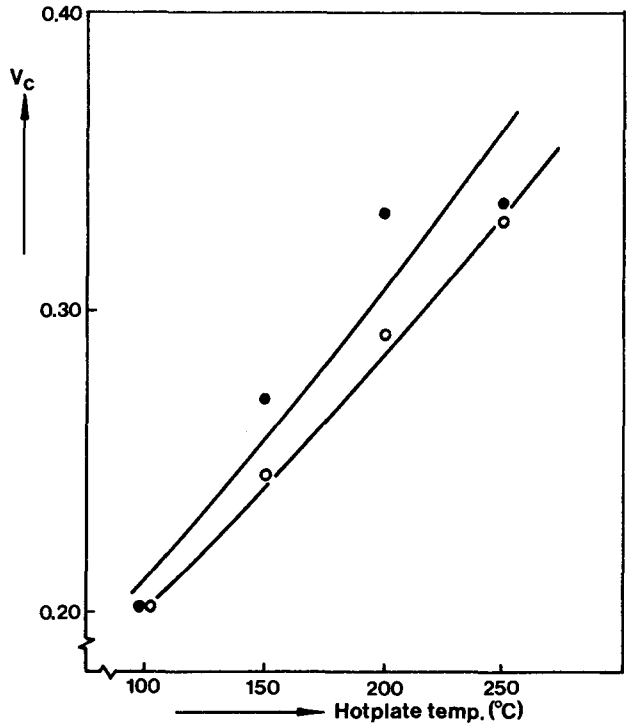

Fig. 8. Crystallinity vs. hot-plate temperature at low tension for two annealing times: (○) 1.3 cN/tex; 30 msec; (●) 1.3 cN/tex, 70 msec.

Crystal Sizes

From the half-width of the x-ray reflection, the apparent crystal size perpendicular to that particular crystal plane can be derived. Table I gives the crystal dimensions perpendicular to the planes 010, 100, and $\bar{1}05$, designated by, respectively, Λ^*_{010}, Λ^*_{100}, and $\Lambda^*_{\bar{1}05}$, after the different treatments. In the discussion of these results, first the behavior of the lateral dimensions Λ^*_{010} and Λ^*_{100} will be treated; after that, the behavior in the fiber direction, i.e., $\Lambda^*_{\bar{1}05}$, will be examined. There is a clear effect of the annealing time on the value of the lateral crystal size.

An example for Λ^*_{010} at low tension is sketched in Figure 11, but it also applies to the lateral crystal size in the other direction, Λ^*_{100}, and at the higher load. This effect, combined with the observation that the dimensions of the unit cell are almost independent of the duration of the heat treatment, shows that the process of alignment of new molecules on the existing surfaces of the crystal is not yet completed within the heat treatment periods used (30 and 70 msec). The distances at which the molecules are built into the crystal, however, reach their equilibrium value almost instantaneously.

There is also a small but definite effect of the applied tension on the lateral crystal growth. This effect is not depicted graphically but examination of the results in Table I clearly shows that high tension favors the lateral growth of the crystals.

The difference is very interesting in the behavior between Λ^*_{010} and Λ^*_{100}. Figure 12 shows an example of such a comparison for low tension and long residence time. It is clear that the growth in the direction perpendicular to the 010

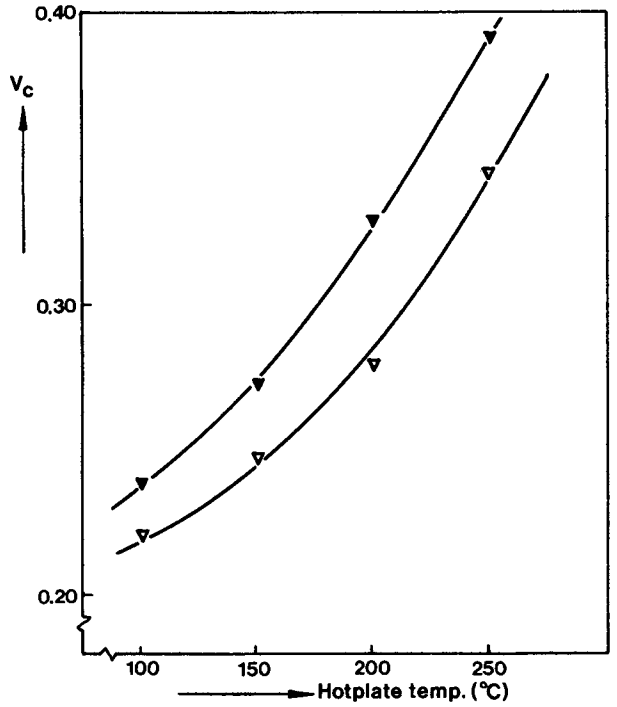

Fig. 9. Crystallinity vs hot-plate temperature at high tension for two annealing times: (▽) 9.2 cN/tex, 30 msec; (▼) 9.2 cN/tex, 70 msec.

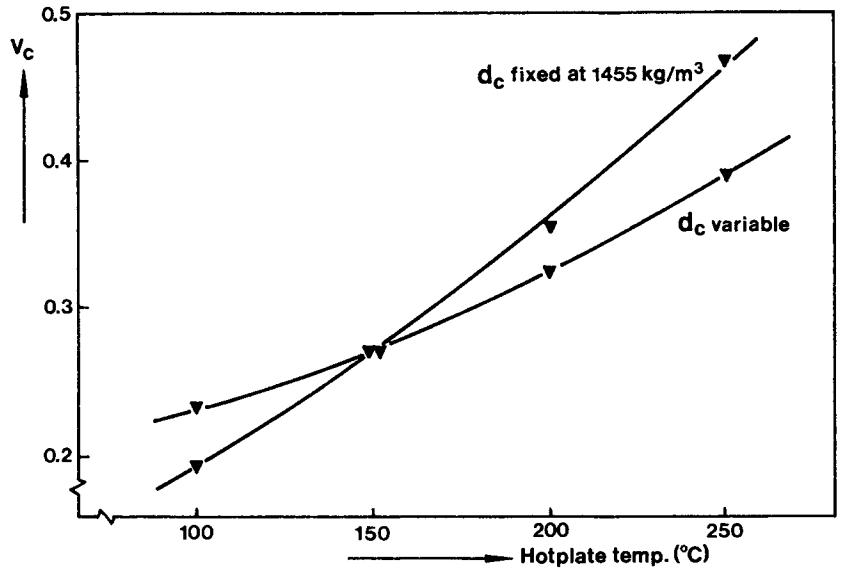

Fig. 10. Comparison of crystallinities calculated with constant and variable crystalline density: (▼) 9.2 cN/tex, 70 msec.

plane is stronger than in the other direction. This effect is also found under the other process conditions (Table I) and in many other samples not used in this investigation.

An explanation of this effect can be given in terms of the reported different

TABLE I
Apparent Crystal Size in Three Directions after Different Process Treatments

Annealing time, msec	Tension, cN/tex	Temperature, °C	Λ^*_{010}, Å	Λ^*_{100}, Å	$\Lambda^*_{\bar{1}05}$, Å
		100	31	36	53
		150	36	31	57
	1.3				
		200	47	37	63
		250	65	47	78
30					
		100	30	29	45
		150	37	32	51
	9.2				
		200	49	40	56
		250	75	53	35
		100	26	21	54
		150	37	32	60
	1.3				
		200	56	41	65
		250	81	56	82
70					
		100	26	31	44
		150	38	33	49
	9.2				
		200	55	41	36
		250	84	58	37

interactions between molecules of poly(ethylene terephthalate). It was found that the dipole–dipole interactions between adjacent ester groups, i.e., along the b-axis (see Fig. 4), is stronger than the interaction via the aromatic π-electrons of the benzene groups.[4,7,8] The observed direction of the strongest growth is the one in which the intermolecular interaction between ester dipoles exists. So the (re)crystallizing polymer system attempts to reach its minimum energy by preferred crystallization in the direction of the strongest interaction. A similar effect has been found by us in an investigation[9] made on nylon 6; in this system, the crystal growth is most pronounced in the direction where the hydrogen bonds are located.

Whereas the applied tension has only a slight effect on the lateral growth of the crystal, a substantial influence is found in longitudinal direction. In Figure 13, the size of the crystal perpendicular to the plane $\bar{1}05$ is shown after the different heat treatments at a tension of 1.3 cN/tex. The direction of the normal of the $\bar{1}05$ plane makes an angle of about 10° with respect to the chain axis, so $\Lambda^*_{\bar{1}05}$ is not exactly the height of the crystal, however, the deviation is less than 2%. As can be seen in Figure 13, an increasing height is found at increasing temperatures; there is also a slight effect of the annealing time.

Figure 14 gives the same parameter but now at a higher load. The observed low values of the eventual crystal height at high temperatures are striking. The reason for this behavior is not quite clear, but these observations may be combined with the observed decrease in chain folding after annealing at high tension reported by Statton et al.[10] This combination gives rise to the conclusion that crystal growth in the direction of the fiber axis is related to the occurrence of regular chain folding.

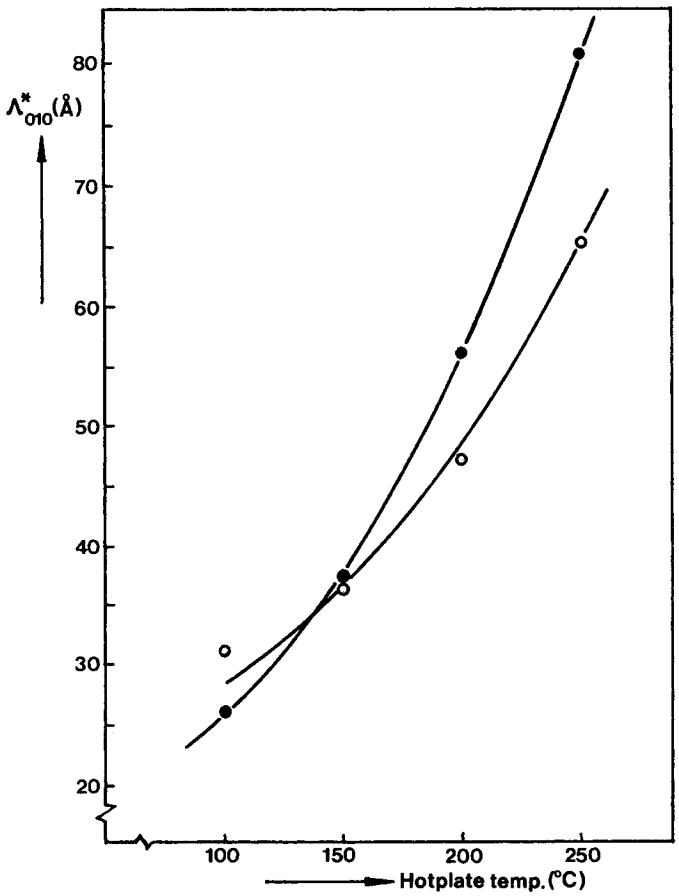

Fig. 11. Dependence of the lateral crystal size Λ^*_{010} vs applied hot-plate temperature at low tension for two annealing times: (○) 1.3 cN/tex, 30 msec; (●) 1.3 cN/tex, 70 msec.

Morphology of the Yarn

The crystallite dimensions in three defined directions being known, the mean volume of these crystals can be calculated. A combination of this volume with the crystallinity yields the total number of the crystals. Figures 15 and 16 give, respectively, volume and number of the crystals at the various temperatures for the case of low tension and long annealing time. While the applied temperature has proved to be the main factor for the development of the eventual structure, in this section only the results for the conditions just mentioned will be discussed. For the other conditions, very similar curves are found. The behavior is clear; in the structures formed at high temperatures, the number of crystals is relatively low, whereas the mean volume is large; at low temperatures, many small crystals are found. This result is in agreement with a model proposed in the literature by Illers and Breuer,[13] who postulated in a study on the dynamic properties of PET the existence of many small crystals at low crystallinity and fewer but bigger ones at a high degree of crystallization.

With the information obtained above, some (semi)quantitative estimates can be made of the volume of the amorphous regions in the fibrils. If it is supposed that there are only fibrils with alternating crystalline and amorphous regions, the calculation of the volume of the amorphous regions is a straightforward one,

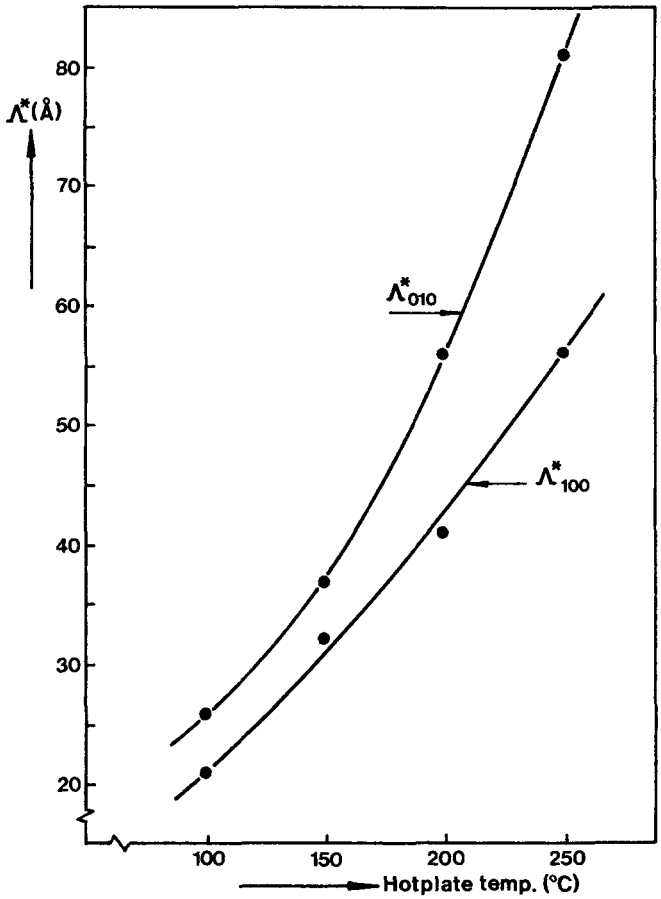

Fig. 12. Different temperature dependence of the two lateral crystal sizes: (●) 1.3 cN/tex, 70 msec.

resulting in

$$\text{Vol}_{\text{amorph.}} = \frac{1 - V_c}{V_c} \text{Vol}_{\text{crys.}}$$

where V_c is volume fraction of crystalline material. The average volumes of the individual amorphous regions thus calculated are given in Figure 17.

The question now is whether this is a fair approximation. For the particular yarns under discussion, values for the long period are determined by means of small-angle x-ray scattering. For that yarn heat treated at 100°C, a well-detectable intensity was not found; for the other three temperatures, long periods of 131, 135, and 149 Å, respectively, were found. These values can be compared with the height of the crystals to obtain an estimate of the crystallinity in the fibril:

$$V_{c\ \text{fibril}} = \frac{\Lambda^*_{\bar{1}05}}{LP}.$$

It is not quite justified to compare values of the crystal height and long period, because the first parameter is not corrected for lattice distortion. However, basing themselves on the experience gained with many PET samples, Dumbleton and Murayama[14] report a correction in the order of 1%. This means that the

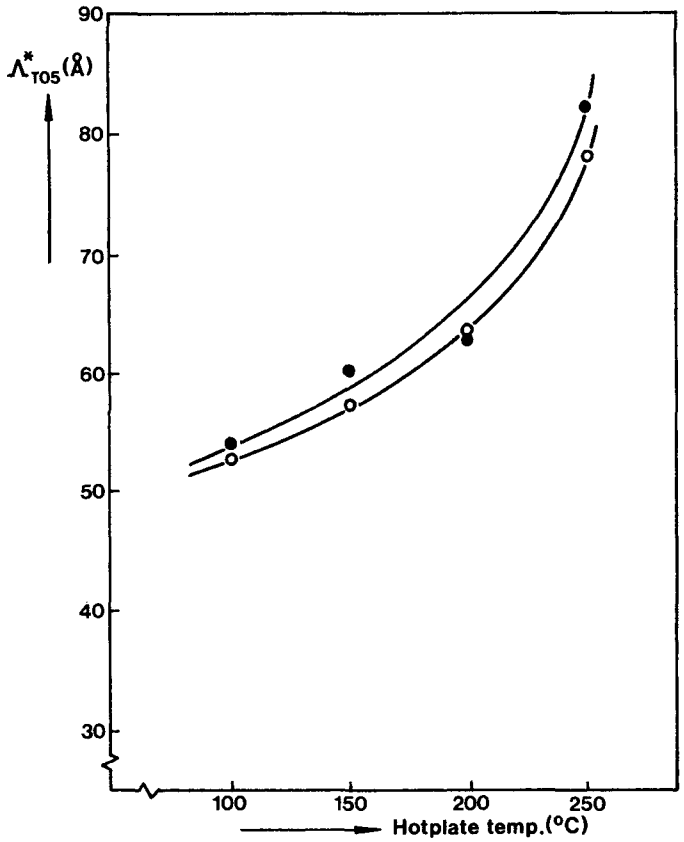

Fig. 13. Height of the crystals at low tension: (○) 1.3 cN/tex, 30 msec; (●) 1.3 cN/tex, 70 msec.

comparison of both parameters mentioned gives a reasonable estimate of the crystallinity within the fibril.

The thus obtained crystallinity within the fibril is higher than the overall crystallinity observed, so that extra amorphous material must be located outside the fibrils. This suggests the existence of an amorphous matrix in which the fibrils are embedded, which was also concluded in the work of Prevorsek et al.[15] According to our present observations, the volume fraction of the matrix is in the order of 30%.

This result has, of course, consequences for the volume of the amorphous regions in the fibrils. These regions will become smaller, for the situation under discussion, by about one half. However, the effect of the temperature on the resulting structure is nearly identical with that sketched in Figure 17. Therefore, despite the uncertainties in the calculation of the volume of the amorphous regions, it is clear that this volume is larger in structures made at higher temperatures. The eventual structures after treatment at low and high temperatures are compared in Figure 18.

Summarizing, it can be stated that increasing temperatures lead to higher crystallinities and bigger crystals for situations of identical annealing times and tensions. Although the total amount of amorphous material decreases with increasing temperatures, the volume of the individual amorphous regions in the fibrils increases.

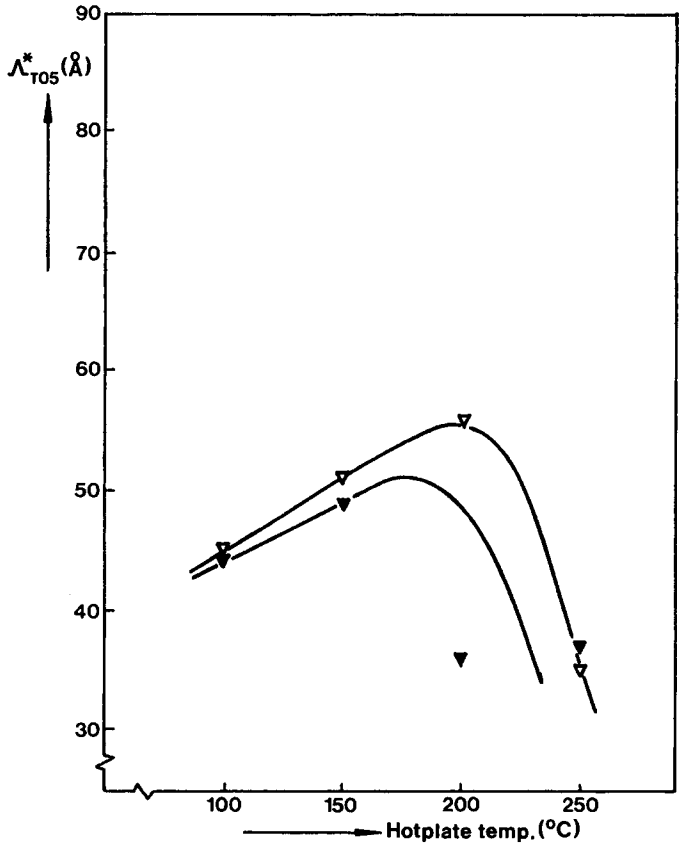

Fig. 14. Height of the crystals at high tension: (▽) 9.2 cN/tex, 30 msec; (▼) 9.2 cN/tex, 70 msec.

ORIENTATION

Both crystalline and overall orientation of the yarns were determined. Crystalline orientation was measured by azimuthal scanning of the reflection $\bar{1}05$. The two overlapping peaks were analyzed by means of curve resolution. From this information, the crystalline orientation factor was calculated by means of the method of Hermans et al.[16] The results are in Table II. The overall orientation was determined by means of pulse propagation. Combination of overall and crystalline orientation can yield information about the orientation of the molecules in the amorphous regions. This method, developed by Samuels,[17,18] was applied to the present series of yarns, using values given by Dumbleton[19] for the moduli of crystalline and amorphous unoriented PET fibers. The resulting orientation factors for the amorphous regions are given in Table II. These data have been used for the estimation of the variation of the amorphous densities as discussed before.

Both amorphous and crystalline orientation factors are plotted in Figure 19 as a function of temperature for the two tension levels and the long annealing time. As can be seen, an improved orientation of the crystals is found when higher crystallization temperatures are used together with a decreased amorphous orientation. Apparently, at higher temperatures a stronger relaxation of the molecules in the amorphous regions will occur. Figure 19 also shows the

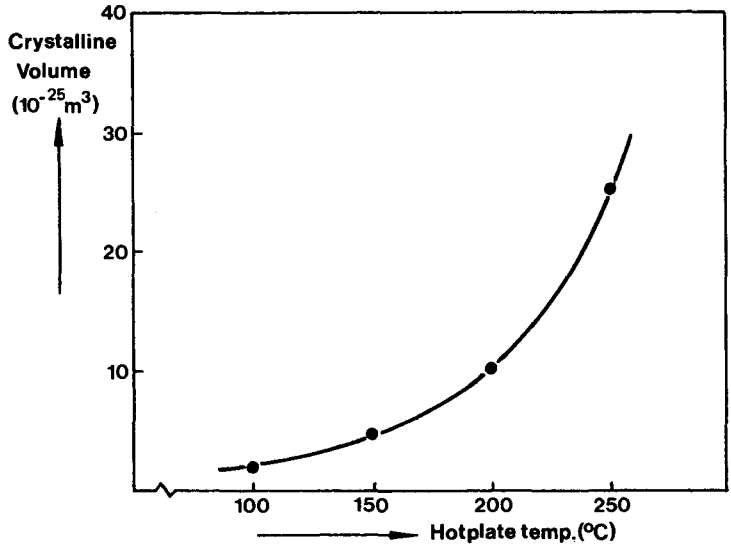

Fig. 15. Volume of the crystals vs hot-plate temperature: (●) 1.3 cN/tex, 70 msec.

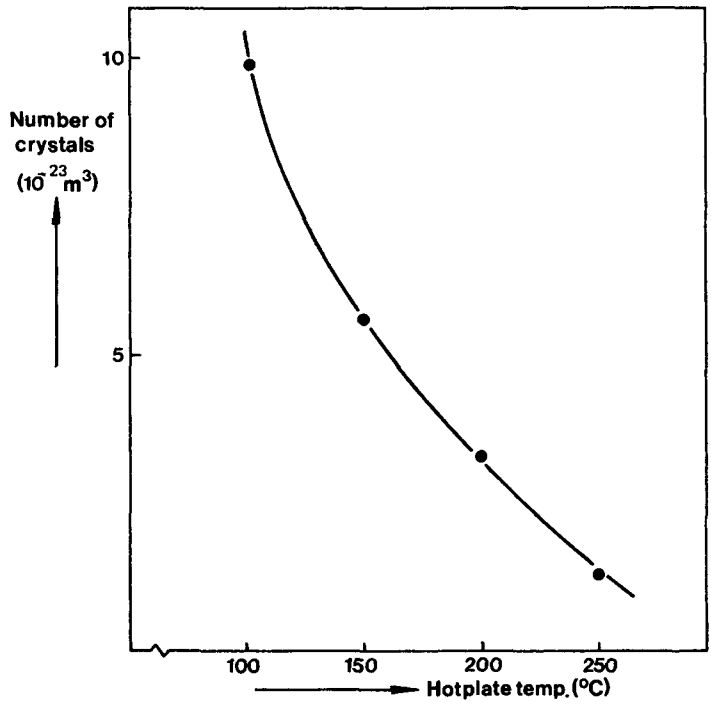

Fig. 16. Number of crystals at different settings of the hot-plate temperature: (●) 1.3 cN/tex, 70 msec.

crystalline orientation to be nearly independent of the tension level within the range investigated. In contrast to this, the effect of the tension on the amorphous orientation is evident.

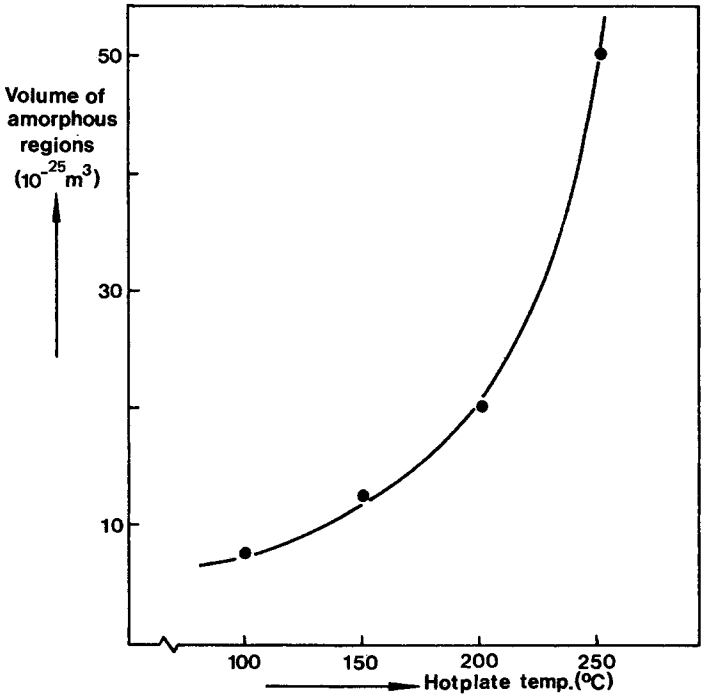

Fig. 17. Volume of the individual amorphous regions vs hot-plate temperature: (●) 1.3 cN/tex, 70 msec.

DYEING BEHAVIOR

The dyeing experiments were carried out under the conditions mentioned in the experimental part of this paper, using Palanilbrilliantred and Foronblue as a high- and a low-energy dye, respectively (dyes with a large and a small molecule). In this section, only some preliminary work will be discussed and interpreted. As the applied temperature is by far the most important factor in controlling the eventual yarn structure, the effect mainly of this parameter will be discussed.

The dye uptake curves for the two dyes are given in Figures 20 and 21. Especially in the case of Palanilbrilliantred, the well-known dip for PET, first reported by Marvin,[20] is observed. In the other picture, the minimum is less pronounced. The dye molecules will, via a diffusion process, only be taken up in the amorphous phase. Therefore, the total volume of the amorphous regions, i.e., the value of $1 - V_c$, must be one of the main factors, governing the dye uptake of a yarn.

In our opinion, another controlling factor will be the accessibility of the amorphous regions. This accessibility will be directly coupled with the mobility of the molecular segments in the amorphous regions. If the crystallites are considered as physical crosslinks decreasing the segmental mobility, as was also suggested in a study of dynamic properties by Illers et al.,[13] many small crystallites will have a greater crosslinking effect than fewer bigger ones. So the accessibility of the amorphous regions can be supposed to be related to their volume.

Therefore, the coarseness of the structure, as discussed before, will have implications for the dyeing behavior. Accordingly, the accessibility to the dye

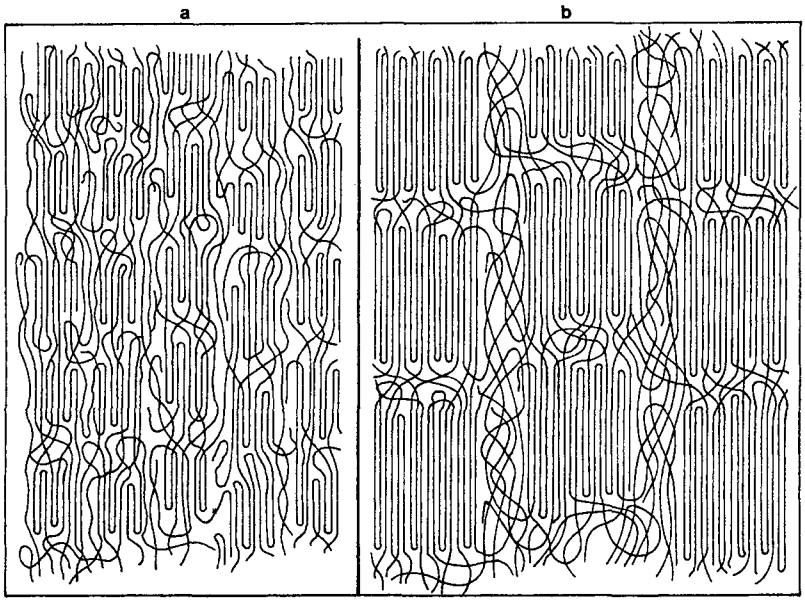

Fig. 18. Comparison of different yarn structures formed: (a) at low temperature; (b) at elevated temperature.

TABLE II
Orientation Data

Annealing time, msec	Tension, cN/tex	Temperature, °C	Orientation factors[a] f_{cr}	f_a
		100	0.927	0.76
		150	0.968	0.71
	1.3	200	0.966	0.68
		250	0.984	0.65
30				
		100	0.901	0.75
	9.2	150	0.959	0.75
		200	0.982	0.76
		100	0.893	0.76
		150	0.970	0.69
	1.3	200	0.977	0.66
		250	0.982	0.63
70				
		100	0.893	0.78
	9.2	150	0.970	0.75
		200	0.979	0.70
		250	0.989	0.66

[a] f_r is crystalline orientation factor; f_a is amorphous orientation factor.

molecule will be great for the coarse structures as obtained by annealing at high temperatures. An indication of the increased segmental mobility in this kind of yarns is found in the work of Statton et al.,[10] who observed in wide-line NMR signals an increased fluid-like mobility in the yarns annealed at elevated temperatures.

Thus, in our model the effect of increasing the annealing temperature consists

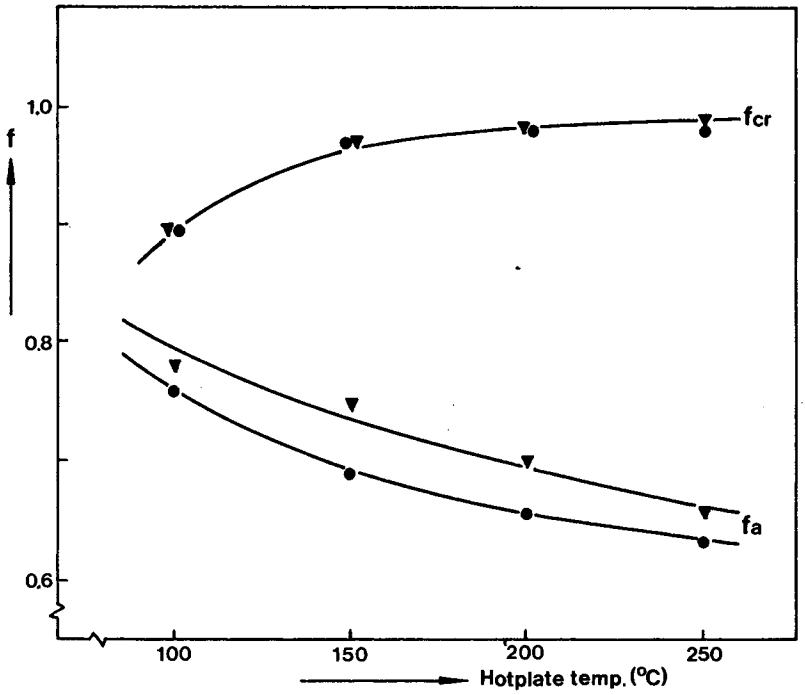

Fig. 19. Crystalline and amorphous orientation factors vs hot-plate temperature: (●) 1.3 cN/tex, 70 msec; (▼) 9.2 cN/tex, 70 msec.

of two opposite factors, i.e., a decrease in the amorphous content, reducing the dye absorption, and an increase in the accessibility facilitating the diffusion of the dyestuff. The balance of these two effects can yield the minimum in dye uptake, as can be observed in Figure 20. A schematic picture of the dyeing model is given in Figure 22, where values for the amorphous content, $1 - V_c$, and the volumes of the individual amorphous regions in the fibrils are given. In the case of Foronblue (Fig. 21), the dye molecule is much smaller. In that situation, the accessibility of the amorphous regions will be a less important factor in the control of the dyeing process than in the case of the big molecule of Palanilbrilliantred. This explains the occurrence of the less pronounced minimum for the low-energy dye Foronblue.

A related model to explain the dyeing behavior of PET yarn was introduced by Gupta, Kumar, and Gulrajani.[21] In their view, an equilibrium will be established between crystallinity and amorphous orientation; less amorphous orientation will promote dyeability. A somewhat similar interpretation was given recently by Braun et al.[22] They postulate an increasing amorphous orientation at temperatures below 170°C and a decrease above 200°C. This type of behavior of the amorphous orientation could not be confirmed in our investigation. Moreover, in our view, the effect of orientation on the dye uptake can only be a second-order one. In the dye bath, the molecules in the amorphous regions will relax almost instantaneously to the equilibrium orientation under the dyeing conditions applied. Only in those cases where the amorphous orientation in the yarn is lower than the equilibrium value corresponding to the dyeing conditions applied can the amorphous orientation have an effect upon the dye uptake of a yarn.

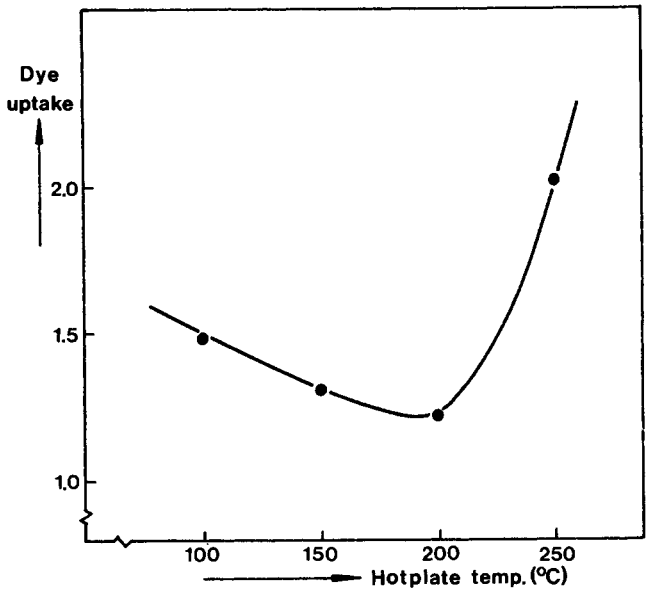

Fig. 20. Uptake of Palanilbrilliantred of yarns heat treated at different temperatures: (●) 1.3 cN/tex, 70 msec.

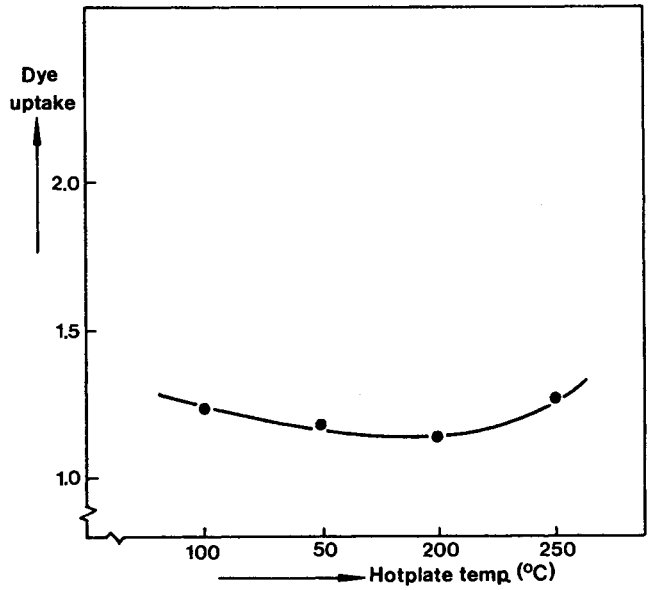

Fig. 21. Uptake of Foronblue of yarns heat treated at different temperatures: (●) 1.3 cN/tex, 70 msec.

Summarizing, we state that the dye uptake of a yarn is controlled by two structural parameters, viz., the total amount of amorphous material and the volumes of the individual amorphous regions. With this model, a reasonable qualitative description can be given of the dyeing behavior of PET yarns. A quantification of these views is the subject of present investigations.

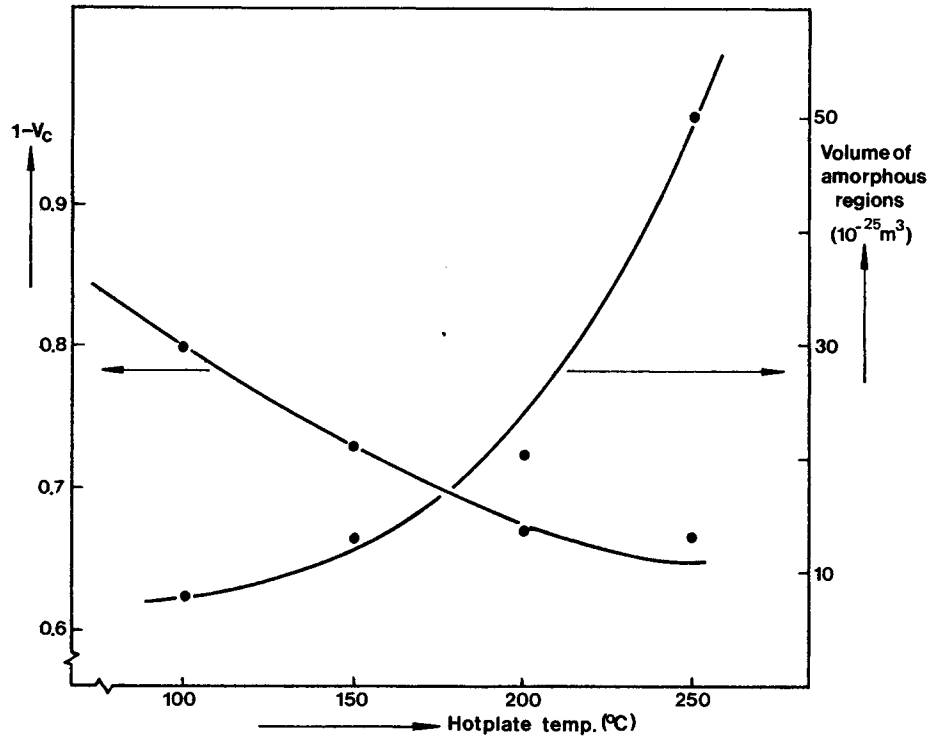

Fig. 22. Schematic representation of the model for description of the dye uptake of PET yarns: (●) 1.3 cN/tex, 70 msec.

CONCLUSIONS

In the investigation described in this paper, efforts have been made to obtain quantitative information about the structure of PET yarns as a function of varying heat treatments of different duration and at different levels of tension. From the results, some main conclusions can be drawn:

(1) The lengths of the unit-cell axes a, b, and c are not constant but depend on the setting of the process variables. Heat treatment at high temperatures results in a better lateral packing of the molecules. The variation in unit-cell dimensions can be interpreted physically.

(2) As a consequence of the first conclusion, the crystalline density is not a constant but depends on the conditions under which the structure is formed. Especially after annealing at high temperatures, a much higher density is found for PET than is usually assumed in the literature. This may give rise to rather large discrepancies between crystallinities calculated with a variable and with constant crystalline density.

(3) The variations of the amorphous density resulting from varying amorphous orientations caused by the different annealing temperatures can be neglected with respect to the corresponding variations of the crystalline density.

(4) The size of the crystals depends on the conditions under which they have grown. Heat treatment at low temperature results in many small crystals. Heat treatment at elevated temperature yields few but bigger crystals. Also annealing time and tension have their influence on the eventual size of the crystals.

(5) The dyeability of a PET yarn can be interpreted in terms of crystalline

morphology. The dye uptake is governed by the total amount of amorphous material and by its accessibility to the dyestuff molecule. This latter factor can be described by structural parameters.

The authors wish to express their thanks to Mr. R. Kooderings Clemens for making the series of annealed yarns and to Mrs. Lenie Adolfsen, Mrs. Marjan Nijpjes, Mr. H. J. v.d. Ven, and Mr. V. Bantwal Rao for their help in experimental structural work. Also the help given by Mr. M. Mannee with computer calculations and by Mr. G.P.T. Vonk in performing the dyeing experiments is gratefully acknowledged.

References

1. H. M. Heuvel, R. Huisman, and K. C. J. B. Lind, *J. Polym. Sci. Polym. Phys. Ed.*, **14,** 921 (1976).
2. L. E. Alexander, *X-Ray Diffraction Methods in Polymer Science,* Wiley-Interscience, New York, 1969, pp. 77–82.
3. H. P. Klug and L. E. Alexander, *X-Ray Diffraction Procedures,* Wiley, New York, 1954, p. 500.
4. R. de P. Daubeny, C. W. Bunn, and C. J. Brown, *Proc. R. Soc. (London),* **A226,** 531 (1954).
5. S. Fakirov, E. Fischer, and G. F. Schmidt, *Makromol. Chem.*, **176,** 2459 (1975).
6. G. Shuck, unpublished results.
7. R. Bonart, *Kolloid-Z. Z. Polym.*, **213,** 1 (1966).
8. E. Liska, *Kolloid-Z. Z. Polym.*, **251,** 1028 (1973).
9. R. Huisman and H. M. Heuvel, *J. Polym. Sci. Polym. Phys. Ed.*, **14,** 941 (1976).
10. W. O. Statton, J. L. Koenig, and M. Hannon, *J. Appl. Phys.*, **41,** 4290 (1970).
11. G. Hinrichsen, *Kolloid-Z. Z. Polym.*, **250,** 1162 (1972).
12. J. H. Nobbs, D. I. Bower, and I. M. Ward, *Polymer,* **17,** 25 (1976).
13. K. H. Illers and H. Breuer, *J. Colloid Sci.*, **18,** 1 (1963).
14. J. H. Dumbleton and T. Murayama, *Kolloid-Z. Z. Polym.*, **220,** 41 (1967).
15. D. C. Prevorsek, G. A. Tirpak, P. J. Harget, and A. C. Reimschluessel, *J. Macromol. Sci., Phys.*, **B9** 733 (1974).
16. J. J. Hermans, R. H. Hermans, D. Vermaas, and A. Weidinger, *Rec. Trav. Chim.*, **65,** 427 (1946).
17. R. J. Samuels, *J. Polym. Sci.*, **A3,** 1741 (1965).
18. R. J. Samuels, *Structured Polymer Properties,* Wiley, New York, 1974, pp. 57–63.
19. J. H. Dumbleton, *J. Polym. Sci.*, **A2, 6,** 795 (1968).
20. D. N. Marvin, *J. Soc. Dyers Colour.*, **70,** 16 (1964).
21. V. B. Gupta, M. Kumar, and M. L. Gulrajani, *Text. Res. J.*, **45,** 463 (1975).
22. P. Braun, S. Müller, F. Osterloh, and H. Zimmermann, *Chemiefasern/Textilind.*, **26,** 550 (1976).

Received December 13, 1976